

Mechanical Reshaping of Inorganic Nanostructures with Weak Nanoscale Forces

Sarah M. Rehn¹, Theodor M. Gerrard-Anderson¹, Liang Qiao¹, Matthew R. Jones^{,1,2}*

¹ Department of Chemistry, Rice University, Houston, Texas 77005, United States.

² Department of Materials Science and NanoEngineering, Rice University, Houston, Texas 77005, United States.

Keywords: nanoplate, post-synthetic modification, nanomechanics, deformation, curvilinear, nanostructure

ABSTRACT

Inorganic nanomaterials are often depicted as rigid structures whose shape is permanent. However, forces that are ordinarily considered weak can exert sufficient stress at the nanoscale to drive mechanical deformation. Here, we leverage van der Waals (VdW) interactions to mechanically reshape inorganic nanostructures from planar to curvilinear. Modified plate deformation theory shows that high aspect ratio 2D particles can be plastically deformed via VdW forces. Informed by this finding, silver nanoplates were deformed over spherical iron oxide template particles, resulting in distinctive bend contour patterns in bright field (BF) transmission electron microscopy (TEM) images. High resolution (HR) TEM images of deformed areas reveal the presence of highly

strained bonds in the material. Finally, we show the distance between two nearby template particles allows for the engineering of several distinct curvilinear morphologies. This work challenges the traditional view of nanoparticles as static objects and introduces methods for post-synthetic mechanical shape control.

MAIN TEXT

Nanoscience is predicated on the idea that properties are dictated by nanoscale structure in the form of particle size and shape.¹ Most often, structure control is exerted either during the synthesis to generate a desired particle morphology, or post-synthesis to site-specifically remove/deposit material or assemble building blocks into superstructures.²⁻⁸ Absent among these strategies is the possibility to physically re-shape or re-form particles via mechanical forces rather than chemical manipulation.⁹⁻¹¹ Previous reports have investigated the mechanical properties of nanomaterials through nanoindentation and other *in situ* methods.¹²⁻¹⁹ However, these approaches are low-throughput, single-particle techniques that are often focused more on measuring mechanical properties than exercising structural control. Nanoparticle flexibility has been observed in certain nanostructures, but often as a consequence of random sample preparation processes.²⁰⁻²² The mechanisms driving deformation, their size dependence, and the ability to create new morphologies via flexibility remain unclear.

Here, we show that ubiquitous van der Waals (VdW) interactions, which are often considered weak compared to most nanoscale forces, can be leveraged to mechanically deform inorganic nanostructures as a means of post-synthetic shape control. To explore the feasibility of this method, a mathematical model was developed based on continuum mechanics theories for

plate deformation. Using the conclusions from this analysis, we show the ability to control the shape of high aspect ratio silver nanoplates by deforming them over small iron oxide template nanospheres. The local deformation caused by a single template particle can therefore be used as a structural motif to create several unique curvilinear structures. This work challenges the conventional notion that nanoparticles are rigid objects and introduces a new class of curvilinear nanostructures.

To understand the forces that might result in nanoparticle deformation, we assumed that typically weak VdW interactions could be leveraged in a situation in which plate-shaped particles interacted with a surface, since this geometry maximizes the VdW contact area compared to other particle shapes. Additionally, we chose to work with noble metal nanoparticles as they are known to be particularly ductile and can readily be synthesized into 2D morphologies.^{20, 23-25} To probe the response to a mechanical stressor under these conditions, Kirchhoff-Love plate theory was employed, which models the elastic deformation and stress behavior of two-dimensional structures. In this formalism, an equilibrium state of mechanical stress is described by a fourth-order partial differential equation, to which there are few tractable solutions. One of the simpler analytical solutions assumes the axially symmetric deformation of a circular disk under a concentrated load (Figure 1a, inset). Modifying this solution to account for plastic deformation allowed us to compare the relative strength of VdW interactions and mechanical strain energy experienced by nanoplates (see Supporting Information). Given some reasonable assumptions, this analysis demonstrates that plates with a thickness of ~ 20 nm and an aspect ratio of ~ 50 represent a transition point, beyond which VdW interactions are capable of causing a significant particle shape transformation (Figure 1a, see Supporting Information).

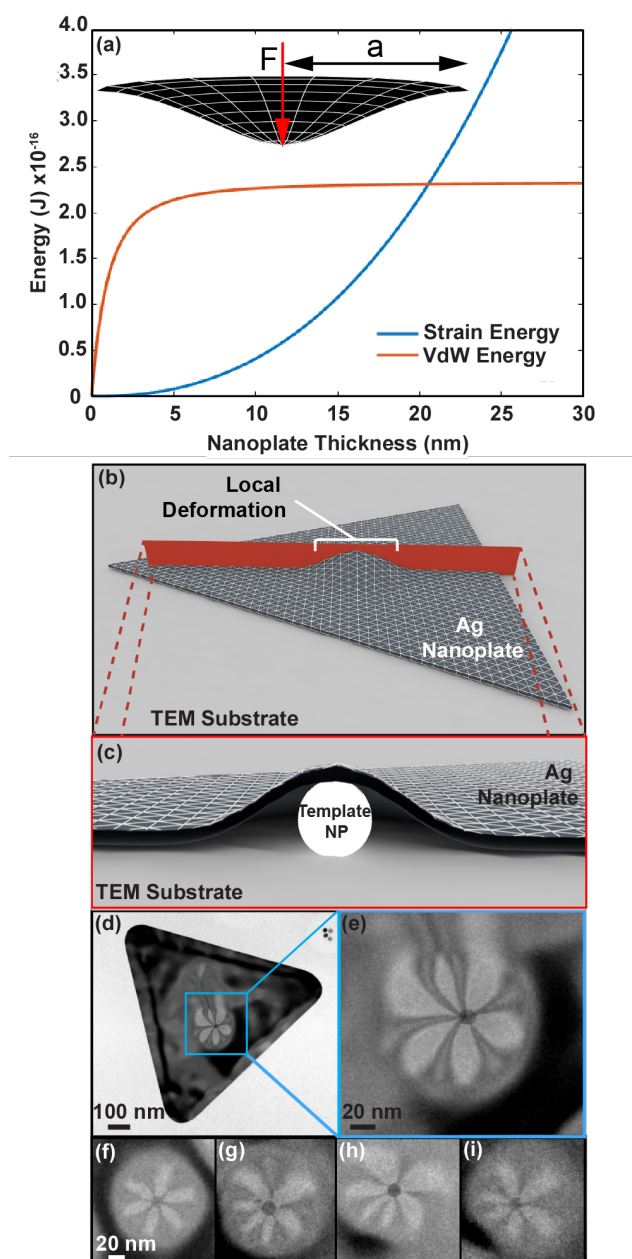


Figure 1. Deformation of thin, silver nanoplates over spherical template particles. (a) Thickness-dependence of the VdW and strain energies as calculated by modified Kirchhoff-Love plate theory. Inset shows the geometry of the strain energy calculation, where F is the concentrated force and a is the disk radius. Schematics of the (b) top-down and (c) cross sectional view for a nanoplate deformed over a spherical template particle. (d) Representative TEM image of a silver nanoplate deformed over one template nanoparticle, (e) a closer look at the unique bend contour that is observed and f-i) several examples of the bend contours that were seen in every instance of a deformed structure.

Importantly, the mathematical solution describing plate deformation used above can be translated to and investigated in an experimental context. High aspect ratio silver nanoplates were synthesized and deformed over spherical iron oxide template particles to mimic a concentrated, axially-symmetric load (Figure 1a inset, 1b-c).^{24,25} The resulting regions of mechanical strain are evidenced by six-lobed deformation patterns in BF TEM data (Figure 1d-e). The unusual pattern of contrast, known as a bend contour, was seen in every instance in which a nanoplate was conformally draped over a spherical template (Figure 1f-i). Bend contours are a phenomenon that occur when local strain causes nearby crystallographic planes to change their orientation and diffraction condition, resulting in variations in contrast.^{20, 26-28} Although bend contours are well-known features of thin TEM samples, they most often extend over large distances and represent gradual changes in the orientation of the material's lattice. The highly symmetric and punctate nature of the bend contours observed in our samples is unusual and points to a localized stress gradient surrounding the spherical particle template. The diameter of these bend contours extended about an order of magnitude larger than the size of the template itself (103 ± 11 nm, $n=228$), validating the assumption of a point load in the plate theory model (Figure 1a).

To confirm whether the 6-fold symmetry of the observed bend contours is related only to an electron diffraction effect and not a real-space morphological feature, we performed selected area electron diffraction (SAED) and dark-field (DF) TEM image analysis. The SAED of a deformed nanoplate exhibits a set of six spots closest to the transmitted beam that represent the $1/3\{422\}$ forbidden reflection which is a known feature of structures with internal twinning (Figure 2a-b).²⁹ The brighter set of six spots represents the first order diffraction from $\{220\}$ planes that reveal distinct deformation lobe pairs when selected for DF TEM imaging (Figure 2c-h). Therefore, the bend contours that appear in BF TEM images are the convolution of symmetric

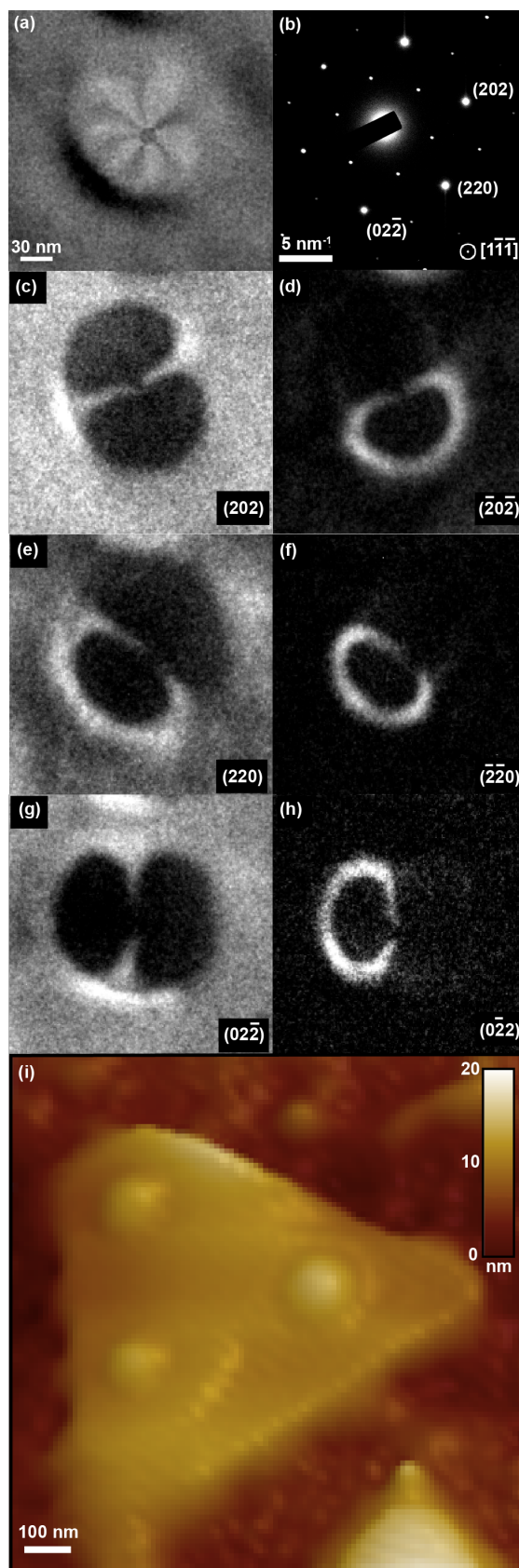


Figure 2. Selected area electron diffraction and dark field analysis of bend contours. (a) BF TEM image of the bend contour used for further analysis. (b) Indexed SAED of the deformed nanoplate revealing the expected $1/3 \{422\}$ diffraction spots arising from twinning along with first order $\{220\}$ diffraction spots, and (c-h) DF TEM images corresponding to these spots. (i) 3D AFM topographical map of a nanoplate with axially-symmetric deformed areas.

deformation lobes occurring via $\{220\}$ planes because the nanoplate is oriented along the $[1\bar{1}\bar{1}]$ zone axis (Figure 2c-h). Atomic force microscopy (AFM) topographical maps show smooth, axially-symmetric features around template-based deformed regions and are in agreement with bend contour sizes measured by TEM (Figures 2i, S9). This confirms that the geometry of the proposed model based on plate theory is appropriate for understanding nanoscale shape control.

If the proposed source of energy to create mechanical stress is VdW interactions, the size of a deformed region should vary based on the contact area between a nanoplate and the substrate. To test this hypothesis, numerous bend contour sizes were measured as a function of the location of the template particle; when positioned near the center of a nanoplate, templates generated bend contours with an average size of 91 ± 7 nm ($n=22$), but when positioned near an edge or a tip of a nanoplate, templates generated bend contours with an average diameter of 103 ± 8 nm ($n=83$). This indicates that with a greater contact area between the particle and the substrate surrounding a template, VdW interactions are cumulatively larger and can exert more mechanical deformation, resulting in smaller bend contours. Conversely, when the template particle is closer to an edge or a tip, there is less surface area available for attractive interactions and the extent of deformation is larger. These data further support the claim that VdW interactions are the primary driving force in the deformation of thin nanoplates.

Because the curvilinear morphology created by the deformation of nanoplates tilts crystallographic planes, it necessarily also strains the atomic lattice. In order to understand the extent of bond strain and whether plastic deformation occurs, we imaged the deformed region surrounding a template particle using HRTEM (Figure 3). Fast-Fourier Transform (FFT) analysis showed a set of six spots that appear more diffuse in the radial direction compared to the analogous spots in the experimental SAED (Figure 3c). This reflects the presence of a range of different bond strain values. To quantify this, three different masks (red, green, blue) were placed at different radial positions over a diffuse spot in the FFT to denote different interatomic distances (Figure 3c, inset). Inverse FFTs generated from these masks allowed for the creation of real-space maps denoting degrees of bond strain in the crystal and range from unstrained (red) to most strained (blue) (Figure 3c-f). From the measured lattice spacing of each mask, a range of tensile strain values could be calculated, revealing bond distances 4.9-7.5% greater than normal in the most deformed regions. This indicates a degree of strain above what is ordinarily considered elastic, confirming the necessity of including plastic deformation in the model for nanoplate mechanics.³⁰⁻

³² It is worth noting that there still exist regions of elastically-strained bonds throughout the structure that are consistent with what has been observed to transform a normally inactive noble metal surface to one that can catalyze chemical reactions.³³⁻³⁵ This suggests that such curvilinear nanostructures might have a high density of active sites for catalysis.

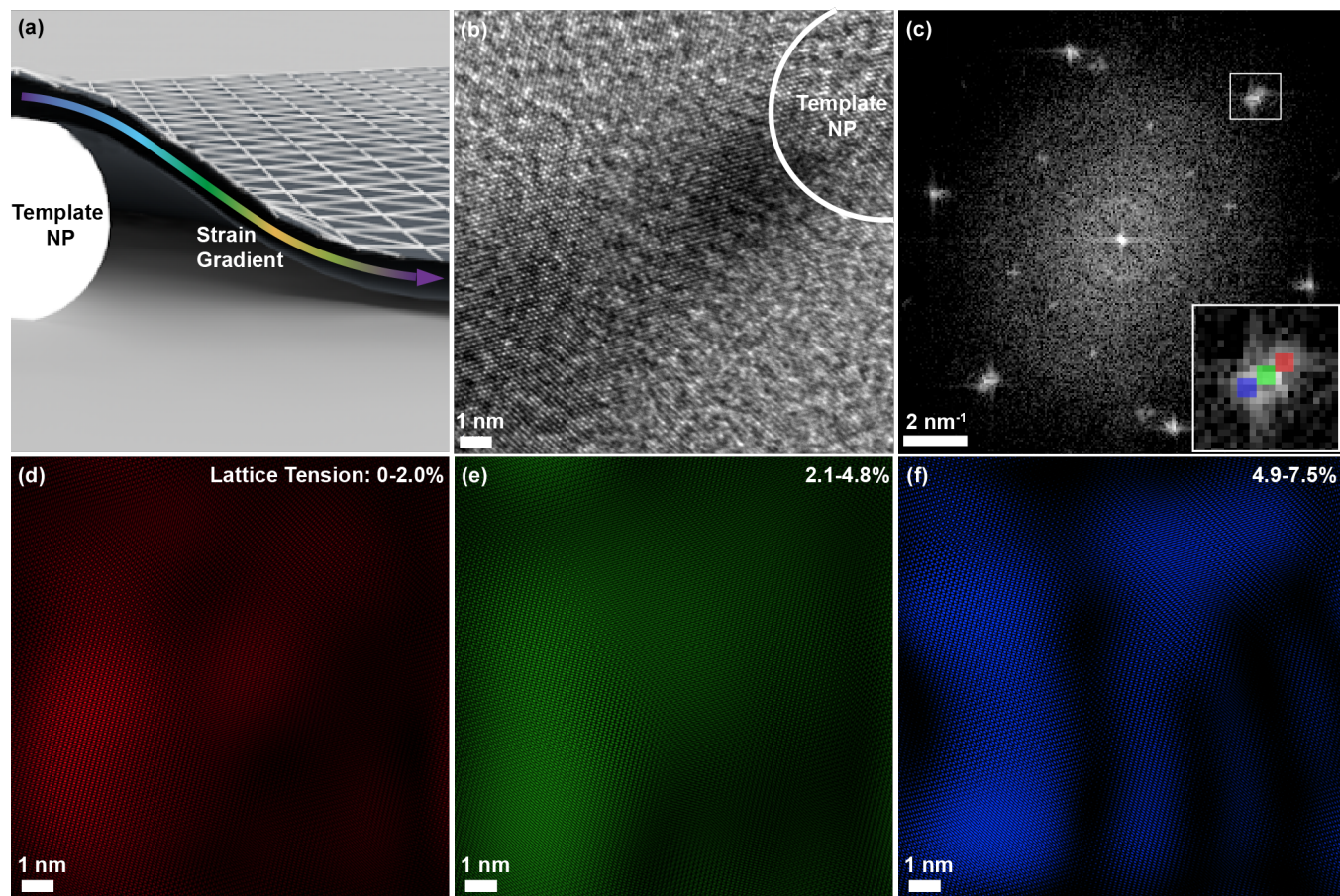


Figure 3. High-resolution TEM analysis of bond strain gradient. (a) Schematic demonstrating the area of bond strain surrounding a template particle. (b) The HRTEM image collected from the strained region near a template particle (upper right) and (c) the corresponding FFT. The inset shows mask placement in the FFT for the calculation of tensile strain. (d-f) Inverse FFT's for each mask demonstrating the progression of tensile strain from least to greatest.

In traditional nanoscale systems, there are canonical structures from which more complex architectures can be built (e.g., spheres assembled into a superlattice or rods lithographically fabricated into metamaterial arrays).^{7, 36} Similarly, we imagined the morphology associated with a single template particle might serve as a basic structural motif for building more complex curvilinear structures. In order to achieve this, we have investigated the topographies that result when two template particles are near one another and deformed regions overlap (Figure 4). If the

parameter d is defined as the spacing between nearby template spheres, $d = 16\text{-}31$ nm generates a single bend contour that appears slightly larger than one associated with a single template particle (Figure 4a). Two templates that are separate but closely spaced ($d = 37\text{-}65$ nm) show a distorted six-lobed pattern with a region bridging the two particles (Figure 4b). Interestingly, when d increases to $\sim 70\text{-}93$ nm, a saddle point is observed, consisting of areas of high lattice compression between particles and lattice tension over the template peaks (Figure 4c). Lastly, templates that are greater than ~ 94 nm apart display bend contours that are completely decoupled from one another (Figure 4d). This method relies on the mutual mechanical relaxation of neighboring deformation fields and opens up the possibility for complex curvilinear architectures based on substrate topography rather than lithographic patterning.

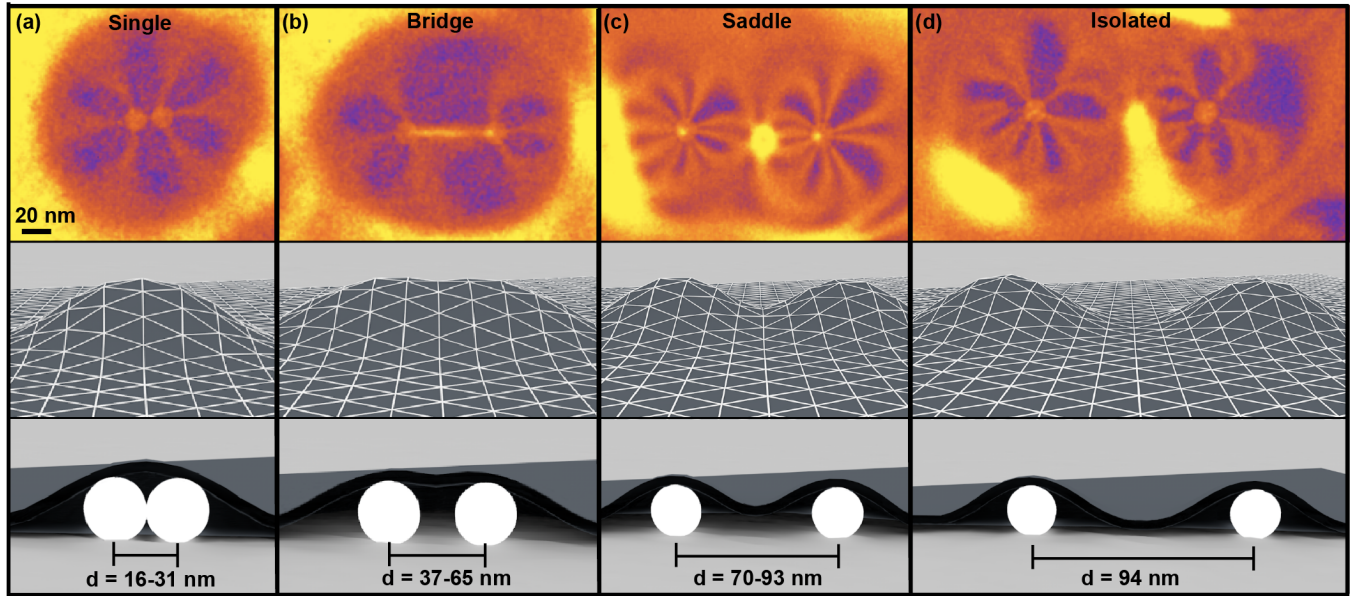


Figure 4. Engineering of coupled curvilinear structures. (a) A single bend contour is observed when two template particles are in physical contact or are extremely close to one another. As two template particles move a distance, d , apart from one another, (b) a single distorted bend contour with a bridged region is observed that eventually becomes (c) two distinct contours with a saddle point between them. (d) Eventually, the two templates are far enough apart that isolated bend

contours are present with complete structural relaxation between them. A colormap was applied to BF TEM images to enhance differences in contrast for the purpose of analysis (Figure S11).

In this work we report a simple method for post-synthetic nanoparticle shape modification via mechanical deformation rather than chemical manipulation. Calculations using Kirchhoff-Love plate theory modified to account for plastic deformation create a framework from which to understand the interplay of forces that facilitate this new type of morphological control. In conjunction with experimental findings, we demonstrate that weak VdW forces can indeed generate enough energy to drive mechanical strain and thereby create a new class of curvilinear structures based on substrate topography. Since these objects would be difficult to generate lithographically, they are expected to result in previously inaccessible electromagnetic modes relevant to the nanooptics community.^{37, 38} Furthermore, the gradient of strained bonds in these materials has implications for their performance or study in catalytic systems.^{33-35, 39} Overall, this work demonstrates that inorganic nanoparticles may be thought of as being capable of dynamic structural changes, actuated by simple and ubiquitous nanoscale forces.

ASSOCIATED CONTENT

Supporting information is available free of charge at:

Experimental details regarding materials and methods, mathematical derivation and calculations, and characterization data.

AUTHOR INFORMATION

Corresponding Author

*Corresponding author. Email:mrj@rice.edu

Author Contributions

The manuscript was written through contributions of all authors. All authors have given approval to the final version of the manuscript.

Funding Sources

Notes

The authors declare no competing financial interest.

ACKNOWLEDGMENT

M. R. J. would like to acknowledge financial support from the Robert A. Welch Foundation (Grant C-1954-20180324). S.M. R. would like to acknowledge financial support from a National Science Foundation Graduate Research Fellowship #1450681. The authors would like to acknowledge financial support from Rice University.

ABBREVIATIONS

BF, bright field; DF, dark field; FFT, fast-fourier transform; HR, high resolution; SAED, selected area electron diffraction; TEM, transmission electron microscopy; VdW, van der Waals

REFERENCES

1. Mock, J. J.; Barbic, M.; Smith, D. R.; Schultz, D. A.; Schultz, S., Shape Effects in Plasmon Resonance of Individual Colloidal Silver Nanoparticles. *J. Chem. Phys.* **2002**, *116*, 6755-6759.
2. Mulvihill, M. J.; Ling, X. Y.; Henzie, J.; Yang, P., Anisotropic Etching of Silver Nanoparticles for Plasmonic Structures Capable of Single-Particle SERS. *J. Am. Chem. Soc.* **2010**, *132*, 268-274.

3. Rathmell, A. R.; Bergin, S. M.; Hua, Y. L.; Li, Z. Y.; Wiley, B. J., The Growth Mechanism of Copper Nanowires and Their Properties in Flexible, Transparent Conducting Films. *Adv. Mater.* **2010**, *22*, 3558-3563.
4. Singh, G.; Chan, H.; Baskin, A.; Gelman, E.; Repnin, N.; Král, P.; Klajn, R., Self-Assembly of Magnetite Nanocubes into Helical Superstructures. *Science* **2014**, *345*, 1149-1153.
5. Jones, M. R.; Macfarlane, R. J.; Lee, B.; Zhang, J.; Young, K. L.; Senesi, A. J.; Mirkin, C. A., DNA-Nanoparticle Superlattices Formed From Anisotropic Building Blocks. *Nat. Mater.* **2010**, *9*, 913-917.
6. Macfarlane, R. J.; Lee, B.; R., J. M.; Harris, N.; Schatz, G. C.; Mirkin, C. A., Nanoparticle Superlattice Engineering with DNA. *Science* **2011**, *334*, 204-208.
7. Lewis, D. J.; Zornberg, L. Z.; Carter, D. J. D.; Macfarlane, R. J., Single-Crystal Winterbottom Constructions of Nanoparticle Superlattices. *Nat. Mater.* **2020**, *19*, 719-724.
8. Straney, P. J.; Marbella, L. E.; Andolina, C. M.; Nuhfer, N. T.; Millstone, J. E., Decoupling Mechanisms of Platinum Deposition on Colloidal Gold Nanoparticle Substrates. *J. Am. Chem. Soc.* **2014**, *136*, 7873-7876.
9. Kim, Y.; Zhu, J.; Yeom, B.; Prima, M. D.; Su, X.; Kim, J.-G.; Yoo, S. J.; Uher, C.; Kotov, N. A., Stretchable Nanoparticle Conductors with Self-Organized Conductive Pathways. *Nature* **2013**, *500*, 59-63.
10. Kim, Y.; Yeom, B.; Arteaga, O.; Yoo, S. J.; Lee, S.-G.; Kim, J.-G.; Kotov, N. A., Reconfigurable Chiroptical Nanocomposites with Chirality Transfer from the Macro- to the Nanoscale. *Nat. Mater.* **2016**, *15*, 461-468.

11. Gu, X. W.; Ye, X.; Koshy, D. M.; Vachhani, S.; Hosemann, P.; Alivisatos, A. P., Tolerance to Structural Disorder and Tunable Mechanical Behaviour in Self-Assembled Superlattices of Polymer-Grafted Nanocrystals. *Proc. Natl. Acad. Sci.* **2017**, *114*, 2836-2841.
12. Pharr, G. M.; Oliver, W. C., Measurement of Thin Film Mechanical Properties Using Nanoindentation. *MRS Bulletin* **1992**, *17*, 28-33.
13. Panin, A.; Shugurov, A.; Oskomov, K., Mechanical Properties of Thin Ag Films on a Silicon Substrate Studied Using the Nanoindentation Technique. *Phys. Solid State* **2005**, *47*, 2055-2059.
14. Zeng, Z.; Tan, J.-C., AFM Nanoindentation to Quatify Mechanical Properties of Nano- and Micron-Sized Crystal of a Metal Organic Framework Material. *ACS App. Mater. Interfaces* **2017**, *9*, 39839-39854.
15. Lee, C.; Wei, X.; Kysar, J. W.; Hone, J., Measurement of the Elastic Properties and Intrinsic Strength of Monolayer Graphene. *Science* **2008**, *321*, 385-388.
16. Gu, X. W.; Wu, Z.; Zhang, Y.-W.; Srolovitz, D. J.; Greer, J. R., Microstructure versus Flaw: Mechanisms of Failure and Strength in Nanostructures. *Nano Lett.* **2013**, *13*, 5703-5709.
17. Zhang, H.; Lu, Y., Low-Cycle Fatigue Testing of Ni Nanowires Based on a Micro-Mechanical Device. *Exp. Mech.* **2017**, *57*, 495-500.
18. Yu, Q.; Legros, M.; Minor, A. M., In situ TEM Nanomechanics. *MRS Bulletin* **2015**, *40*, 62-70.
19. Patil, R. P.; Doan, D.; Aitken, Z. H.; Chen, S.; Kiani, M. T.; Barr, C. M.; Hattar, K.; Zhang, Y.-W.; Gu, X. W., Hardening in Au-Ag nano boxes from Stacking Fault-Dislocation Interactions. *Nat. Commun.* **2020**, *11*, 2923.
20. Rodríguez-González, B.; Pastoriza-Santos, I.; Liz-Marzán, L. M., Bending Contours in Silver Nanoprisms. *J. Phys. Chem. B* **2006**, *110*, 11796-11799.

21. De, S.; Higgins, T. M.; Lyons, P. E.; Doherty, E. M.; Nirmalraj, P. N.; Blau, W. J.; Boland, J. J.; Coleman, J. N., Silver Nanowire Networks as Flexible, Transparent, Conducting Films: Extremely High DC to Optical Conductivity Ratios. *ACS Nano* **2009**, *3*, 1767-1774.
22. Lee, J.; Lee, P.; Lee, H.; Lee, D.; Lee, S. S.; Ko, S. H., Very Long Ag Nanowire Synthesis and its Application in Highly Transparent, Conductive and Flexible Metal Electrode Touch Panel. *Nanoscale* **2012**, *4*, 6408-6414.
23. Mehl, M. J.; Papaconstantopoulos, D. A.; Kioussis, N.; Herbranson, M., Tight-Binding Study of Stacking Fault Energies and the Rice Criterion of Ductility in the FCC Metals. *Phys. Rev. B* **2000**, *61*, 4894-4897.
24. Zhang, Q.; Li, N.; Goebel, J.; Lu, Z.; Yin, Y., A Systematic Study of the Synthesis of Silver Nanoplates: Is "Citrate" a Magic Reagent? *J. Am. Chem. Soc.* **2011**, *133*, 18931-18939.
25. Liu, X.; Li, L.; Yang, Y.; Yin, Y.; Gao, C., One-Step Growth of Triangular Silver Nanoplates with Predictable Sizes on a Large Scale. *Nanoscale* **2014**, *6*, 4513-4516.
26. Carlton, C. E.; Ferreira, P. J., In Situ TEM Nanoindentation of Nanoparticles. *Micron* **2012**, *43*, 1134-1139.
27. Sun, H.; Pan, X., Microstructure of ZnO Shell on Zn Nanoparticles. *J. Mater. Res.* **2004**, *19*, 3062-3067.
28. Cuberes, M. T.; Stegemann, B.; Kaiser, B.; Rademann, K., Ultrasonic Force Microscopy on Strained Antimony Nanoparticles. *107* **2007**, 1053-1060.
29. Germain, V.; Li, J.; Inger, D.; Wang, Z. L.; Pileni, M. P., Stacking Faults in Formation of Silver Nanodisks. *J. Phys. Chem. B* **2003**, *107* (34), 8717-8720.
30. Zhang, J.; Tang, Y.; Lee, K.; Ouyang, M., Nonepitaxial Growth of Hybrid Core-Shell Nanostructures with Large Lattice Mismatches. *Science* **2010**, *327*, 1634-1638.

31. Yao, Y.; He, D. S.; Lin, Y.; Feng, X.; Wang, X.; Yin, P.; Hong, X.; Zhou, G.; Wu, Y.; Li, Y., Modulating FCC and HCP Ruthenium on the Surface of Palladium-Copper Alloy Through Tunable Lattice Mismatch. *Angewandte Chemie* **2016**, *128*, 5591-5595.
32. Diao, J.; Gall, K.; Dunn, M. L., Yield Strength Asymmetry in Metal Nanowires. *Nano Lett.* **2004**, *4*, 1863-1867.
33. Kim, J.-S.; Kim, H.-K.; Kim, S.-H.; Kim, I.; Yu, T.; Han, G.-H.; Lee, K.-Y.; Lee, J.-C.; Ahn, J.-P., Catalytically Active Au Layers Grown on Pd Nanoparticles for Direct Synthesis of H₂O₂: Lattice Strain and Charge-Transfer Perspective Analyses. *ACS Nano* **2019**, *13* (4), 4761-4770.
34. Bueno, S. L. A.; Gamler, J. T. L.; Skrabalak, S. E., Ligand-Guided Growth of Alloyed Shells on Intermetallic Seeds as a Route Toward Multimetallic nano catalysts with Shape-Control. *Chem. Nano Mat.* **2020**, *6*, 783-789.
35. Mukherjee, D.; Gamler, J. T. L.; Skrabalak, S. E.; Unocic, R. R., Lattice Strain Measurement of Core@Shell Electrocatalysts with 4D Scanning Transmission Electron Microscopy Nanobeam Electron Diffraction. *ACS Catal.* **2020**, *10*, 5529-5541.
36. Pryce, I. M.; Kelaita, Y. A.; Aydin, K.; Atwater, H. A., Compliant Metamaterials for Resonantly Enhanced Infrared Absorption Spectroscopy and Refractive Index Sensing. *ACS Nano* **2011**, *5* (10), 8167-8174.
37. Prodan, E.; Radloff, C.; Halas, N. J.; Nordlander, P., A Hybridization Model for the Plasmon Resonance of Complex Nanostructures. *Science* **2003**, *302*, 419-422.
38. Wang, H.; Brandl, D. W.; Nordlander, P.; Halas, N. J., Plasmonic Nanostructures: Artificial Molecules. *Acc. Chem. Res.* **2007**, *40*, 53-62.
39. Sneed, B. T.; Young, A. P.; Tsung, C.-K., Building up Strain in Colloidal Metal Nanoparticle Catalysts. *Nanoscale* **2015**, *7*, 12248-12265.

